Desalination and Water Treatment
www.deswater.com

doi: 10.5004/dwt.2021.27319

228 (2021) 217–228
July

Magnetic MgAl-LDH: a green nanocatalyst for wet peroxide oxidation of phenol: experimental study and process modeling by response surface methodology and artificial neural network

Masoud Samandari[a], Afshin Taghvamanesh[a,*], Seyed Ali Hosseini[b], Sakineh Mansouri[a]

[a]*Department of Chemistry, Central Tehran Branch, Islamic Azad University, Tehran, Iran, emails: Afshintagvamenesh@gmail.com/ taaf2007@gmail.com (A. Taghvamanesh), m.samandari2009@gmail.com (M. Samandari), taaf2007@gmail.com/ sak.mansouri@iauctb.ac.ir (S. Mansouri)*
[b]*Department of Applied Chemistry, Urmia University, Urmia, Iran, email: a.hosseini@urmia.ac.ir*

Received 5 November 2020; Accepted 2 April 2021

ABSTRACT

Fe_3O_4@MgAl-LDH as a new magnetic nanocatalyst was developed for phenol removal from wastewater in the catalytic wet peroxide oxidation process. It was synthesized by co-precipitation and characterized by X-ray diffraction, Fourier-transform infrared spectroscopy, vibrating sample magnetometer, field-emission scanning electron microscopy/energy-dispersive X-ray spectroscopy, and Brunauer–Emmett–Teller. The results confirmed that Fe_3O_4@MgAl-LDH is a super-magnetic nanocomposite with a specific saturation magnetization (Ms) of 18.63 emu g^{-1} and a specific surface area of 235.8 m^2 g^{-1}. The modelling of the process was done using both response surface methodology (RSM) and artificial neural network (ANN). The Pareto analysis indicated that the relative importance of the process variables is as following: phenol concentration > volume of peroxide > dosage of the catalyst > reaction time. The optimum condition was at 0.5 g L^{-1}, 100 min, 0.7 mL, 65.15 ppm of catalyst amount, reaction time, peroxide volume and phenol concentration, respectively. The predicted response under optimum conditions was 96%, whereas the experimental response resulted in 98%. The feed-forward back-propagation was used for ANN modelling including the topology of 4 input variables, 8 neurons in the hidden layer and 1 output. The training of the network was accomplished by a Levenberg–Marquardt. The mean square error for the ANN and RSM models were 0.22 and 0.87, respectively, and the R^2 values were 0.99 and 0.98, respectively. It is concluded that black-box ANN indicates a higher accuracy in estimating phenol remediation. The study showed that magnetic layered double hydroxides could be a promising catalyst for phenol removal from wastewaters.

Keywords: Layered double hydroxide; Wet peroxide oxidation; Magnetic nanocatalyst; Phenol; Artificial neural network

1. Introduction

Phenol and phenolic compounds are released from various industries such as petrochemical and coking processes [1–3]. The permissible limit of phenol is 1 mg L^{-1} for industrial effluents to be discharged into inland surface waters (IS: 2490–1974) and 5 mg L^{-1} for discharge into public sewers (IS: 3306–1974) [4]. According to the guides of the World Health Organization (WHO), the maximum allowance of phenol in drinking water is 0.002 mg L^{-1}. There are two common methods used to eliminate the phenol contents in wastewater, that is, physical–chemical and biological methods [5–7]. The biological degradation of phenol is hard and it is very toxic so it is necessary to reduce the amount of phenol from wastewater. Biological treatment is environmentally friendly and energy-saving, but it cannot treat high concentration pollutants. Physical and chemical methods generate secondary by-products which eventually enter the environment as toxic aquatic pollutants [1–3,8]. Table 1 summarizes the advantages and disadvantages of physical–chemical methods [9]. The methods are divided

* Corresponding author.

into conventional and advanced methods. The conventional treatments show high efficiencies with various phenolic compounds, while advanced treatments such as photochemical treatment, Fenton processes and wet air oxidation use fewer chemicals compared to the conventional ones but have high energy costs. Through the various chemical methods used for the removal of phenol, its catalytic oxidation by hydrogen peroxide is considered a suitable method. The complete degradation of phenol is resulted from this method at near ambient temperatures [3,10]. Like other catalytic processes, the property of the catalyst affects the efficiency of the process. Recently the use of transition metal catalyst especially, catalysts containing iron and copper have been reported [3,4,10,11].

Layered double hydroxides (LDHs) are the materials containing divalent and trivalent cations and the anions are interlayer [11]. LDH has different applications such as adsorbents of aqueous pollutants. The use of magnetic LDHs could facilitate their removal from the media after the process is finished [12]. Except for adsorption and catalysis, the magnetic catalysts have been used in drug delivery, protein separation, reductive-acetylation of nitroarenes and textile wastewater treatment [13–17].

The objectives of this work were to develop the magnetic Fe_3O_4@MgAl-LDH nanocomposite as a novel magnetic nanocatalyst for remediation of phenol from wastewater using the CWPO process. The process was modelled by both response surface methodology (RSM) and artificial neural network (ANN) techniques to get which one could predict and model the process exactly. RSM is a statistical and mathematical technique useful for modelling and optimizing processes [18–20]. ANN is a black box tool for modelling and optimization. The magnetic LDH was synthesized by co-precipitation and characterized by X-ray diffraction (XRD), Fourier-transform infrared spectroscopy (FTIR), energy-dispersive X-ray spectroscopy, vibrating sample magnetometer (VSM), field-emission scanning electron microscopy (FE-SEM), and Brunauer–Emmett–Teller (BET) techniques.

2. Experimental

The chemicals of NaOH, $FeCl_2{\cdot}6H_2O$, $FeCl_3{\cdot}6H_2O$, Na_2CO_3, $Mg(NO_3)_2{\cdot}6H_2O$ and $Al(NO_3)_3{\cdot}9H_2O$ were purchased from Merck Company and used without further purification.

2.1. Synthesis of MgAl-LDHs

The MgAl-LDH was synthesized using a co-precipitation method. Briefly, metallic nitrates with Mg/Al molar ratio of 1 was dissolved in distilled water. Using the NaOH 2 M, the pH of the solution was adjusted at 9 and CO_3^{2-} was used as an interlayer anion (using 0.02 M Na_2CO_3). The solution was continuously stirred for 2 h and the resulted slurry was aged at 70°C for 12 h. The resulting product was separated by centrifugation, washed twice with distilled water, and then dried at 60°C for 12 h to get LDH [18].

2.2. Synthesis of Fe_3O_4 particles

5.8 g of $FeCl_3$ and 2.15 g of $FeCl_2$ were dissolved in 40 mL of water in an N_2 atmosphere. The solution was stirred for 2 h at 60°C. 5 mL of 28% aqueous ammonia solution was dropwise added to the above solution with continuous stirring until the pH of the solution reached 9.

A black precipitate was formed, which was removed magnetically, washed, and dried at 60°C for 6 h.

2.3. Synthesis of Fe_3O_4@MgAl-LDH

The Fe_3O_4@MgAl-LDH composite was synthesized by the precipitation of the LDH in the presence of the preformed Fe_3O_4 particles. At first, the Fe_3O_4 suspension was prepared by a mixture containing Fe_3O_4 (0.15 g) in 20 mL of deionized water for 5 min. Then the salt solution containing LDH was added dropwise to a suspension of Fe_3O_4 with continuous stirring. As before, the precipitates were separated using centrifugation and washed several times with deionized water. Finally, the magnetic-LDH precipitates were dried at 60°C for a day and heated at 200°C [21,22].

2.4. Characterization of Fe_3O_4@MgAl-LDH

The crystalline phases of the catalyst were investigated by a Philips PW1800 diffractometer and Cu Kα radiation (λ = 1.54 Å). FTIR spectra were recorded on a Bruker

Table 1
Comparison of efficiency and costs of phenol removal techniques

	Methods	Efficiency	Pollutant conc./amount	Cost
Conventional methods	Distillation	High	High	Low
	Extraction	High	Medium	Low
	Absorption/adsorption	High	High	Low
	Biological treatment	High	Low	Low
	Chemical oxidation	High	High	Low
	Electrochemical oxidation	High	Medium	High
Advanced methods	Fenton/electro-Fenton	High	Medium	High
	Ozonation	High	High	Medium
	Wet air oxidation	High	High	Medium
	Photochemical treatment	High	Low	High

spectrometer (model TENSOR 27) at room temperature using the KBr disc technique.

The morphology of the mixed oxides was determined via field-emission scanning electron microscopy (FE-SEM) by a TESCAN MIRA-3 instrument with precoating samples with gold. The mapping of the LDHs film was investigated by a TESCAN electron microscope. The specific surface area of the nanocatalyst was determined using the BET method.

A VSM was used for determining the magnetic properties of the composite and done by Meghnatis Daghigh Kavir VSM. The N_2 adsorption–desorption isotherms were carried out using BELSORP, Japan.

2.5. Experimental process

A batch mode setup was used for the catalytic oxidation process of phenol. The schematic of the setup is shown in Fig. 1. For a typical run, a definite amount of fresh catalyst and hydrogen peroxide (according to the RSM experimental design matrix) was put into a simulated phenolic wastewater under continuous stirring at 500 pm. The sampling from the solution was done at definite time intervals and immediately analyzed. The phenol and product concentration in the wastewater were detected and measured by UV-Vis spectrophotometer. After the process, some MnO_2 was added to the solution to eliminate residual H_2O_2. An External magnet was used to remove the catalyst before measuring the residual phenol.

2.6. Experimental design and modelling procedure

Box–Behnken design of RSM was used to design the experiments and to interpret the effect of the functional factors of phenol concentration, contact time, catalyst dosage and peroxide volume on the responses (phenolic compounds removal %).

The three levels were considered for each variable and a total of 27 runs to run an experiment. The experimental ranges and levels of the independent test variables are presented in Table 2.

3. Results and discussions

3.1. Characterization of Fe_3O_4@MgAl-LDH

Fig. 2 shows the FTIR spectrum of Fe_3O_4@MgAl-LDH composite. For the magnetic composite sample, the strong and broadband centered on 3,435 cm^{-1} is related to stretching vibrations of O–H in the brucite layers and interlayer water molecules [22,23]. The band at 1,637 cm^{-1} corresponds to a water deformation and that at 1,387 cm^{-1} is related to the interaction between the CO_3^{2-} and the OH group [22], indicating that some CO_3^{2-} ions existed inside LDHs. The bands from 400 to 900 cm^{-1} are attributed to the stretching vibration and bending vibration of M–O and M–OH [23]. The strong absorptions at 521 cm^{-1} from the Fe–O lattice vibration of Fe_3O_4 [22]. These results suggest that the Fe_3O_4@MgAl-LDH composite has been achieved successfully.

Fig. 3 shows the XRD pattern of the composite Fe_3O_4@MgAl (1:2) LDH. The characteristic peaks of hydrotalcite-like compounds which are appeared at 11, 23, 34, 38, 46, 59 and 61.5 are observed. So the layered structure of the sample is approved. The peaks of Fe_3O_4 is not observed in the pattern [13]. No other diffraction peaks were not detected; it resulted that the as-prepared Fe_3O_4@MgAl-LDH was a pure composite of Fe_3O_4 with MgAl-LDH.

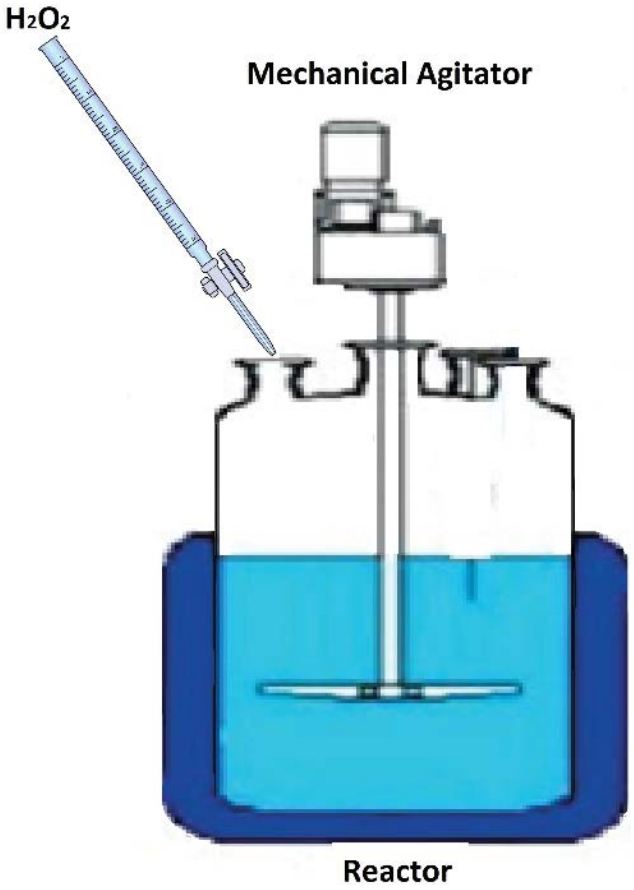

Fig. 1. Scheme of the experimental tests in CWPO process.

Table 2
Experimental ranges and levels of the independent test variables

Variables	Symbol	Ranges of levels		
		–1	0	+1
Catalyst amount (g)	x_1	0.3	0.4	0.5
Phenol concentration (ppm)	x_2	50	125	200
Reaction time (min)	x_3	60	80	100
Peroxide volume	x_4	0.3	0.5	0.7

The VSM curves of Fe_3O_4@MgAl-LDH is shown in Fig. 4. The specific saturation magnetization (Ms) of the catalyst is 18.63 emu g^{-1} and the curve approve that the catalyst is a super-magnetic material [13].

The morphology and particle size of the catalysts was investigated by SEM (Fig. 5). The particles of the catalyst are comprised of sphere-like particles, which the layer morphology is observable on the surface of particles. The SEM image of the catalysts reveals that the mean particle sizes of all catalysts are in nanoscale (less than 100 nm).

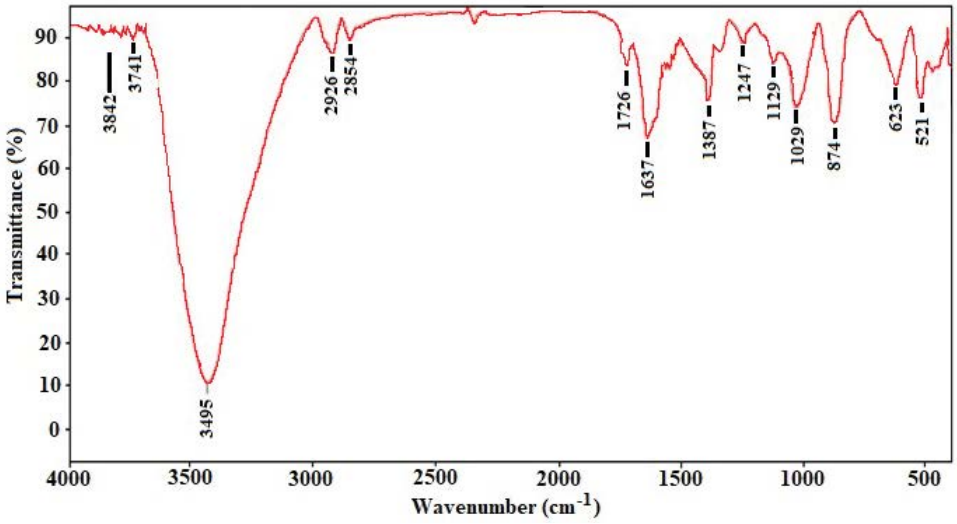

Fig. 2. FTIR spectrum of Fe_3O_4@MgAl-LDH.

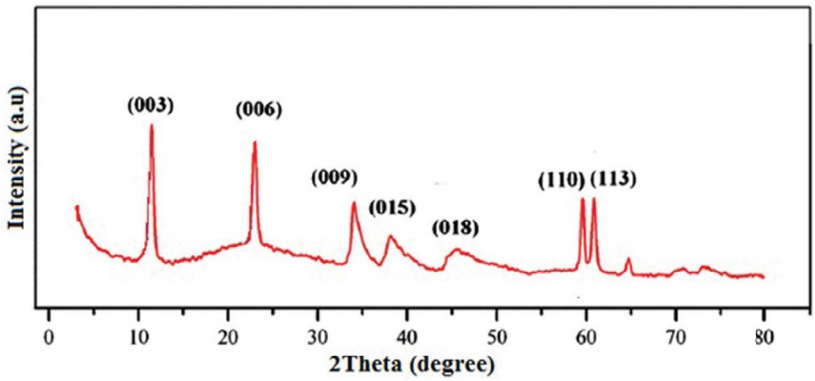

Fig. 3. XRD pattern of the catalyst.

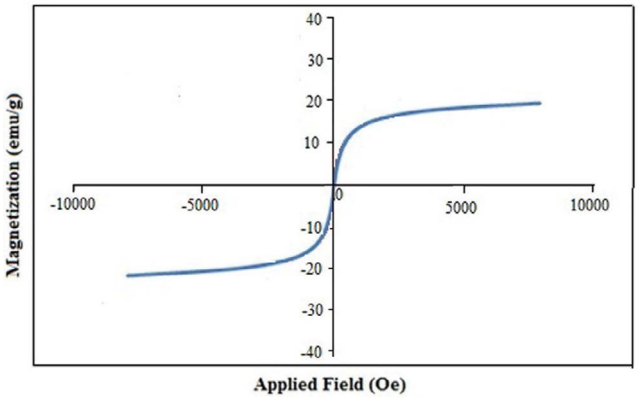

Fig. 4. VSM spectra of the catalyst.

In Fig. 6, the mapping of the catalyst is shown and it is observed that O, Mg, and Fe are uniformly dispersed, regardless of the morphology of the examined region. Thus it is concluded that Fe_3O_4 is uniformly dispersed in the matrix of the catalyst.

The specific surface area of the nanocatalyst determined using the BET method. The pore volume and pore size distribution were derived from the desorption profiles of the isotherms using the Barrett–Joyner–Halenda method. The results indicated that the catalyst has a high relative surface area (235.8 m^2 g^{-1}). The pores of the nanocatalyst were mostly microporous (average diameter of 1.65 nm). The high surface area of the magnetic catalyst has usually a direct relationship with the particle size of the catalyst. The smaller the particle size, the higher the specific surface area [3,14,15,23].

3.2. Results of RSM modelling

The effect of process variables like phenol concentration, contact time, catalyst dosage and peroxide volume on the removal of phenol was investigated using response surface methodology according to Box–Behnken Design. The batch runs were conducted in Box–Behnken designed experiments to visualize the effects of independent factors on responses. Experiments are conducted according to the Box–Behnken experimental design as shown in Table 3.

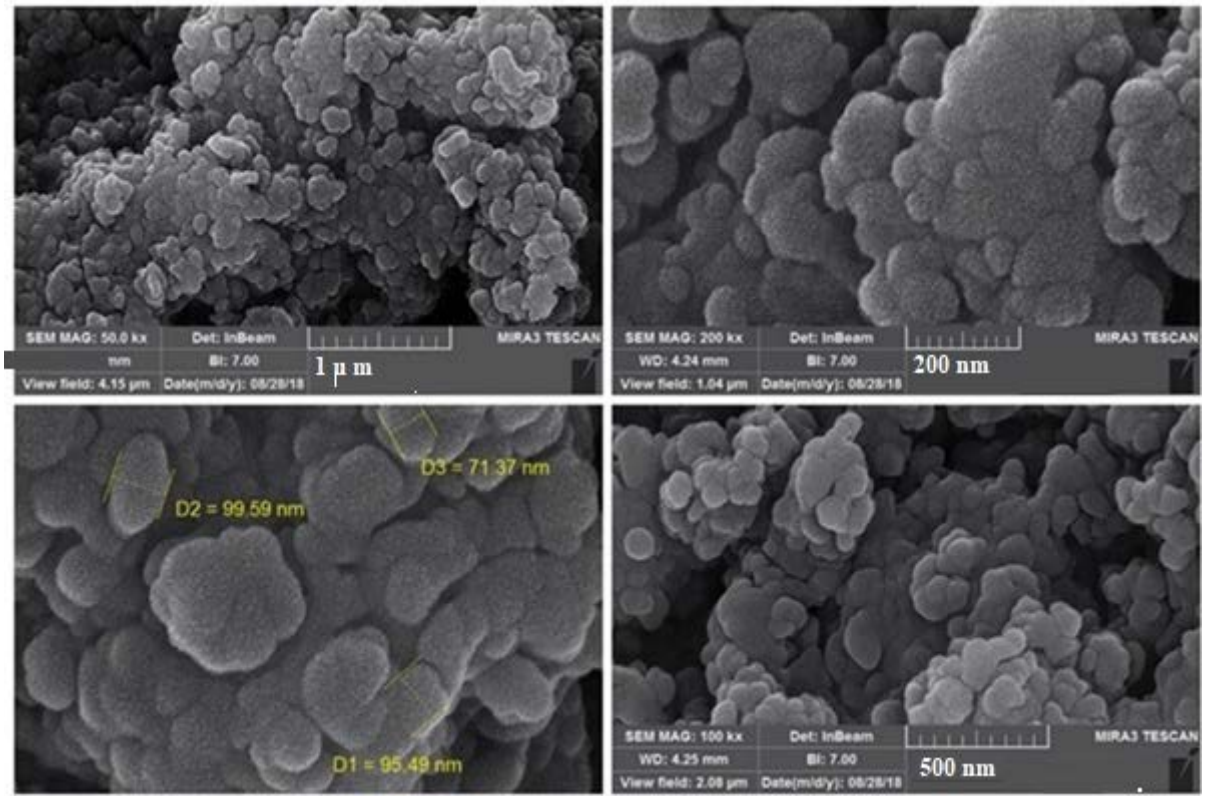

Fig. 5. FE-SEM images of Fe_3O_4@MgAl-LDH.

Multiple regression analysis of the experimental data yielded the following regression equation for the percentage removal of phenol [Eq. (1)].

$$\text{Response} = 238.9 - 302.5\,x_1 + 0.1644\,x_2 - 1.596\,x_3 - 194.8\,x_4 + 287.5\,x_1^2 - 0.000622\,x_2^2 + 0.00813\,x_3^2 + 71.9\,x_4^2 - 0.1667\,x_1x_2 + 225.0\,x_1x_4 + 0.625\,x_3x_4 \quad (1)$$

The model predicts that among singular terms, all factors except the concentration of phenol show a negative effect on the response. Among binary terms, the interaction of x_1x_2 has a negative effect on the response, while x_1x_4 and x_3x_4 term have a positive impact on the response.

Table 4 shows the analysis of variance (ANOVA) for the percentage removal of phenol. Analysis of variance is required to test the significance and adequacy of the model [24–26]. The mean squares are obtained by dividing the corresponding sum of squares by the degrees of freedom. The fisher's variance ratio (F-value) is the ratio of the mean square owing to regression to the mean square owing to an error [24–26]. Here the ANOVA of the regression model demonstrates that the model is highly significant as evident from the calculated F-value (82.59) and a very low probability value (P = <0.0001). The determination coefficient (R^2) is a statistical key factor to investigate the significance of the model. It is a correlation criterion between the experimental and predicted data.

A graph of the phenol removal percentage (experimental response) plotted vs. the predicted responses is exhibited in Fig. 7. The determination coefficient between the predicted and observed values for the conversion was 0.9838, confirming that experimental results are in good agreement with predicted results.

Another proof to approve the efficiency of the models is to evaluate the residuals.

Fig. 8a shows the plot of the predicted response against the residual values (normal probability plot). A graph of the residual against the predicted response shows random behaviour without a tendency to residuals for experimental values (Fig. 8b). Fig. 8c shows the plot of residuals against the order of data shows randomly dispersed around the horizontal axis and accordingly the residual plots approve the adequacy of the model.

Furthermore, the F-test was used to verify the statistical analysis of the model.

It is concluded from the results of the F-test that the model is statistically significant with an F-value of 82.59. The p-value and t-value of each term of the model are shown in Table 5.

Since the p-values of all the coefficients are $P < 0.05$, it implies that these are significant. The linear effect of coefficients main variables is significant ($P < 0.0001$). Similarly, the interactive effects of x_1x_2, x_1x_4 and x_3x_4 as well as the quadratic terms are also significant.

Besides, the relative significance of model terms was predicted by Pareto analysis (according to Eq. (2)) [3]:

$$P_i = \left(\frac{bi^2}{\sum bi^2}\right) \times 100 \left(i \neq 0\right) \quad (2)$$

Table 3
Box–Behnken design matrix along with experimental and predicted response values for phenol removal

						Predicted	
Run order	Catalyst dose (g L^{-1})	Concentration (ppm)	Time (min)	V (H_2O_2) mL	Experimental	RSM	ANN
1	0.4	125	100	0.7	93	93.708	92.887
2	0.4	125	100	0.3	82	81.875	81.967
3	0.5	125	80	0.7	98	96.916	97.697
4	0.3	125	100	0.5	86	85.875	88.743
5	0.4	50	60	0.5	85	85.083	92.919
6	0.4	125	60	0.3	87	86.208	82.038
7	0.5	200	80	0.5	77	77.041	92.788
8	0.4	200	80	0.3	74	72.958	83.04
9	0.4	125	80	0.5	81	81.333	91.26
10	0.3	125	80	0.3	85	86.25	82.344
11	0.4	50	80	0.7	87	88.458	91.455
12	0.4	200	60	0.5	76	76.416	86.886
13	0.3	125	80	0.7	85	84.083	91.85
14	0.4	125	80	0.5	81	81.333	81.127
15	0.5	125	80	0.3	80	81.083	94.979
16	0.4	200	100	0.5	77	77.083	87.576
17	0.3	125	60	0.5	86	85.208	93
18	0.5	50	80	0.5	89	88.208	84.95
19	0.5	125	100	0.5	90	89.041	95.02
20	0.4	125	80	0.5	82	81.333	85.99
21	0.4	50	100	0.5	86	85.75	92.99
22	0.5	125	60	0.5	88	89.041	82
23	0.4	50	80	0.3	82	81.625	94.504
24	0.3	200	80	0.5	75	75.708	85.989
25	0.4	125	60	0.7	88	88.041	81.141
26	0.3	50	80	0.5	82	81.875	91.51
27	0.4	200	80	0.7	80	79.791	81.889

Table 4
Analysis of variance of the proposed model

Source of variations	Sum of squares	Degree of freedom	Adjusted mean square	F-value
Regression	797.500	11	72.500	82.59
Residuals	13.167	15	0.878	
Total	810.667	26		
R^2 = 98.38%	R^2(adj) = 97.18%	R^2(pred) = 93.30%		

The result of the Pareto analysis is shown in Fig. 9. According to the analysis the order for the independent variables as follows:

Phenol concentration > volume of peroxide > dosage of the catalyst > reaction time. Among the main factors, the concentration of phenol and dosage of the catalyst is the most effective factors on the oxidation of the phenol. The result is in agreement with the results of Hosseini et al. [3]. They studied the phenol removal by the CWPO process by consideration 4 process variables and concluded that the phenol concentration is the most important process variable. Gholipoor and Hosseini [23] studied the catalytic wet peroxide oxidation of phenol on Cu-MOF. They optimized the process by considering four variables, that is, reaction temperature, phenol concentration, Cu-MOF dosage and contact time and resulted that the relative importance of phenol removal is as follows: reaction temperature > phenol concentration > Cu-MOF dosage > contact time. Since in our work, the reaction temperature is constant and had not been considered as a process variable, the initial phenol concentration resulted as the most important variable in the CWPO process.

Among the variables, the effects of the main factors on phenol relative importance of the model terms on the

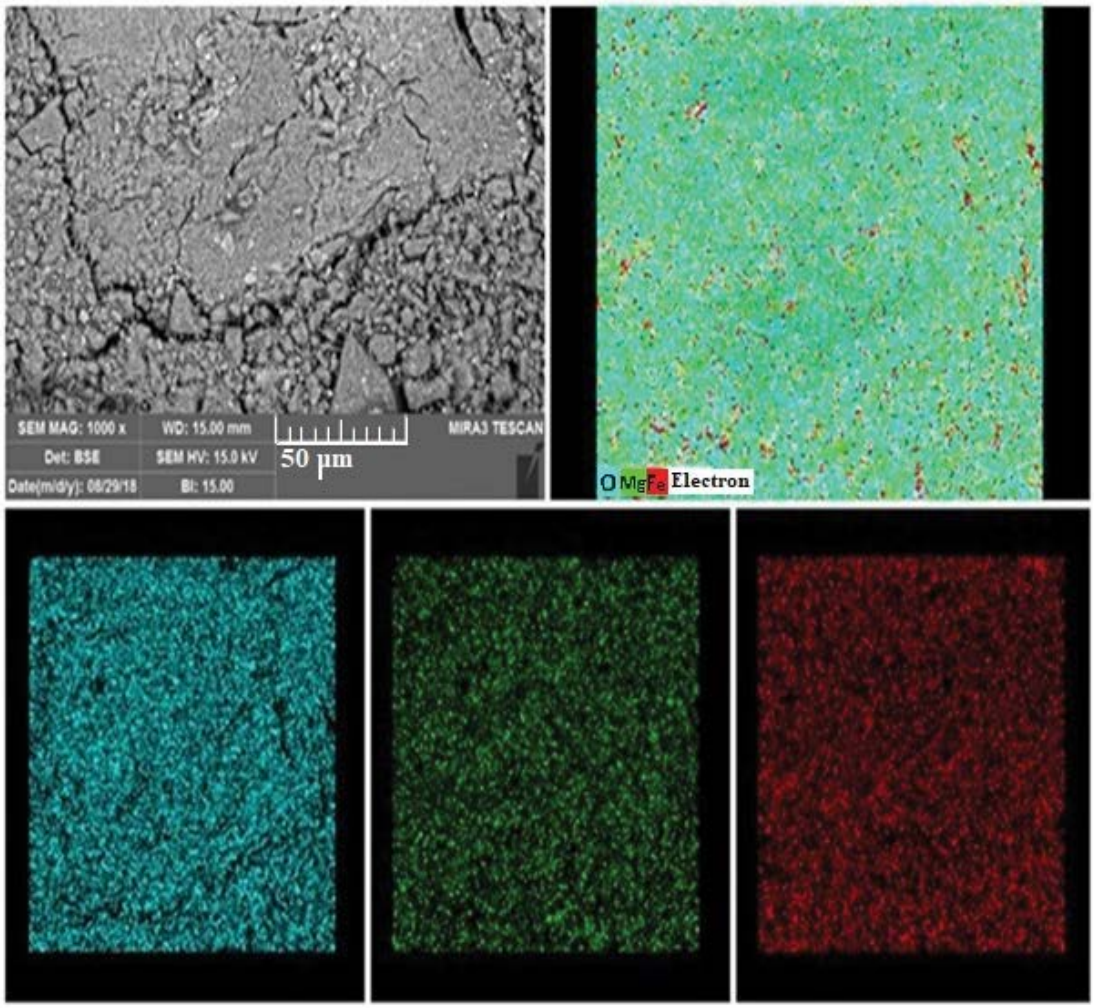

Fig. 6. SEM image, energy-dispersive X-ray spectroscopy mapping.

phenol removal are as following order: x_1x_4 (19.92%) > x_2 (18.47%) > x_2^2 (12.05%) > x_4 (11.48%) > x_3^2 (10.39%) > x_1^2 (8.13%), x_4^2 (8.13%) > x_3x_4 (6.148%) > x_1 (3.16%) > x_1x_2 (1.54%) > x_2 (0.81%) > x_3 (0.1%).

3.3. Response surface plots and optimizing

The relationship between independent and dependent variables as illustrated in three-dimensional (3D) response surface plots and two-dimensional (2D) contour plots.

The three-dimensional response surface and the two-dimensional contour plots are the graphical representations of the regression equation and provide a method for predicting the efficiency of phenol removal with different values of the variables and identification of the type of interactions between these variables.

Each contour curve represents an infinite number of combinations of two variables with the other maintained at their respective zero levels. A circular contour of response indicates that the interaction between the corresponding variables is negligible. In contrast, an elliptical or saddle nature of the contour plots indicates that the interaction between the corresponding variables is significant [24–26].

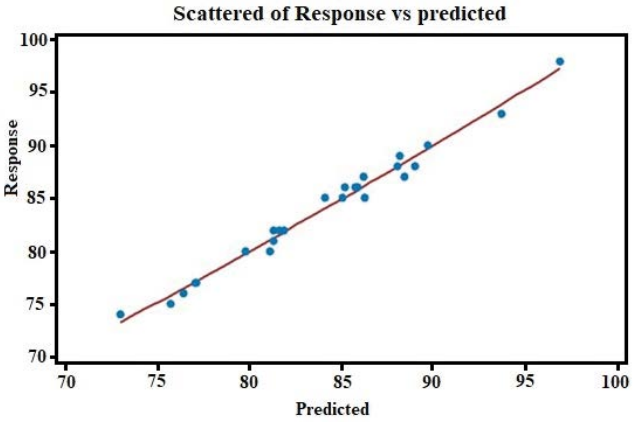

Fig. 7. Correlation between experimental and predicted responses.

Fig. 10 illustrates the three-dimensional (3D) surface plot and 2D contour for the combined interaction of peroxide volume and reaction time on the catalytic wet peroxide oxidation of phenol. As represented in Fig. 10, maximum

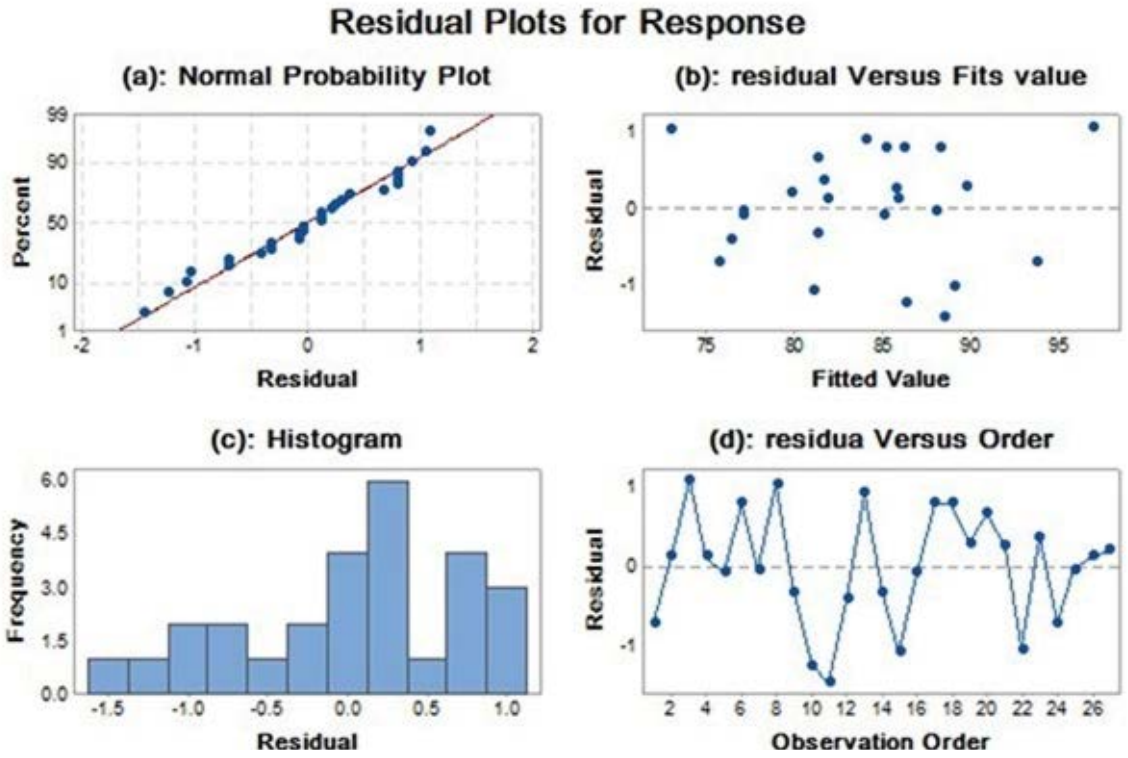

Fig. 8. Residual plots for CWPO of phenol.

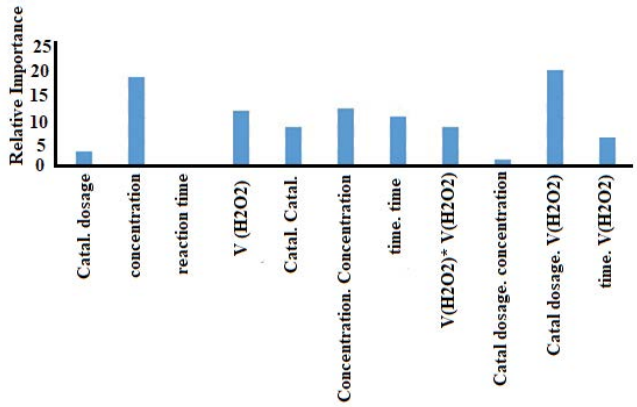

Fig. 9. Results of Pareto analysis.

degradation is at a high level of reaction time and a high level of peroxide volume.

Fig. 11 shows the 2D contour and 3D surface plot for the interaction of catalyst dosage and peroxide volume. The term x_1x_4 exhibited a positive effect on the phenol degradation and it was found from this figure that increasing the amount of both peroxide volume and catalyst dosage leads to maximize the degradation of phenol.

In the case of binary interaction of concentration of phenol and catalyst dosage, as indicated in Fig. 12, the x_1x_2 has a negative effect on the degradation of the phenol and the optimum condition occur at the high-level of catalyst and low concentrations of the phenol, as indicated by dark green section.

Furthermore, the optimum condition for the degradation of the phenol was predicted by the response surface methodology (RSM). The optimum condition was at 0.5 g L^{-1}, 100 min, 0.7 mL, 65.15 ppm of catalyst amount, reaction time, peroxide volume and phenol concentration, respectively. The predicted response under these conditions was 96%, whereas the experimental test of the predicted condition led to 98% degradation for phenol. Gholipoor et al. [23] reported that the optimal conditions for the phenol degradation occurred at phenol concentration 400 ppm, Cu-MOF amount (1.5 g L^{-1}) at 50°C for 30 min with a 91.87% of phenol removal.

3.4. ANN modelling

Artificial neural networks are centred on modelling the process based on the behaviour of brain neurons. Of course, the processes are considerably less complex than the brain, hence ANN is as nonlinear empirical models that are especially useful in representing input-output data, making predictions in time, classifying data, and recognizing patterns [27].

ANNs having a highly interconnected structure, consist of a large number of simple processing elements called neurons, which are arranged in different layers in the networks; an input layer(s), an output layer(s) and hidden layers [27].

Hidden layers perform the non-linear transformations on the input space and computation purpose.

In this study, a three-layered (input, hidden and output) feed-forward back propagation neural network with Levenberg–Marquardt learning algorithm was used for modelling phenol removal from wastewater by catalytic wet

Table 5
Estimated regression coefficient and corresponding *t* and *p*-value

Term	Coefficient	*t*-value	*p*-value
Constant	81.333	150.36	0.000
x_1 (catalyst amount)	1.917	7.09	0.000
x_2 (phenol concentration)	–4.333	–16.02	0.000
x_3 (reaction time)	0.333	1.23	0.237
x_4 (peroxide volume)	3.417	12.63	0.000
$x_1 \cdot x_1$	2.875	7.09	0.000
$x_2 \cdot x_2$	–3.500	–8.63	0.000
$x_3 \cdot x_3$	3.250	8.01	0.000
$x_4 \cdot x_4$	2.875	7.09	0.000
$x_1 \cdot x_2$	–1.250	–2.67	0.018
$x_1 \cdot x_4$	4.500	9.61	0.000
$x_3 \cdot x_4$	2.500	5.34	0.000

Table 6
Comparison between the results of RSM and ANN modeling

Parameters	RSM model	ANN model
Regression coefficient	0.983	0.991
MSE	0.878	0.22
Model developing	With interactions	Without interactions

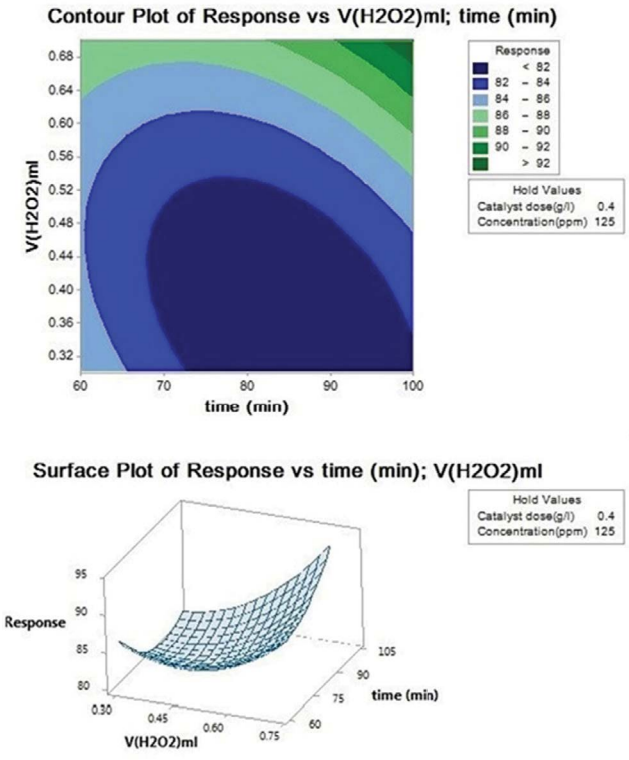

Fig. 10. The 3D surface plot and 2D contour for the combined interaction of peroxide volume and reaction time.

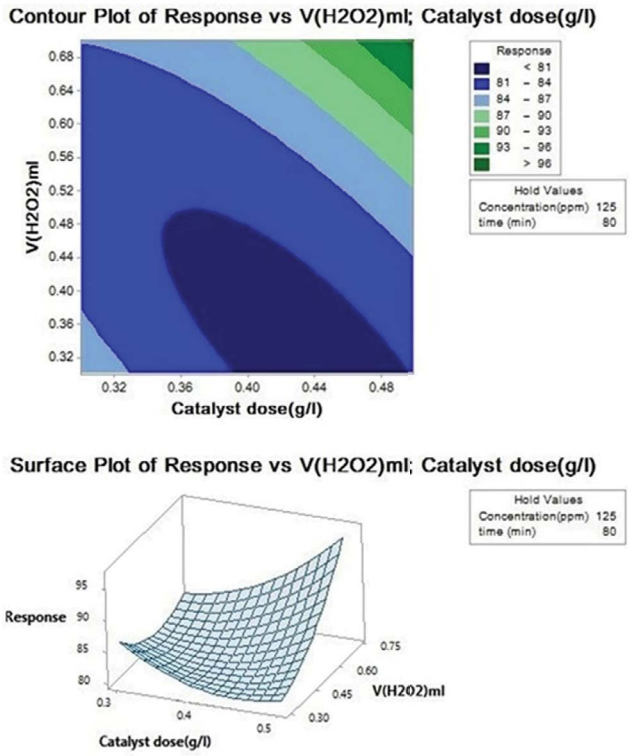

Fig. 11. The 2D contour and 3D surface plot for the interaction of catalyst dosage and peroxide volume.

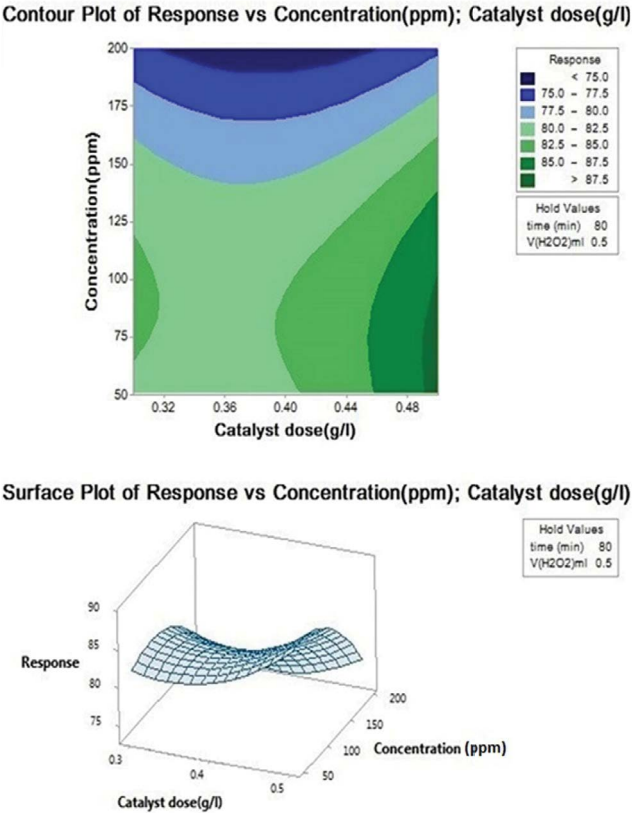

Fig. 12. The 2D contour and 3D surface plot for the interaction of catalyst dosage and concentration.

peroxide oxidation over magnetic LDH as a function of process parameters.

Four input neurons were the phenol concentration, contact time, catalyst dosage and peroxide volume, a single hidden layer of neurons, and an output neuron indicating the percentage of phenol removal. Normalization of the inputs and targets was done in the range of (−1) to (1) to make the neural network training more efficient. The hyperbolic tangent sigmoid transfer function 'TANSIG' was used for the hidden layer while a purely linear transfer function 'PURELIN' was chosen for the output layer. Mean square error (MSE) values were used as the error function. This function measures the network performance using equation 3.

$$\mathrm{MSE} = \left(\frac{\sum_{i=1}^{n} \left(y_{nn} - y_{\exp} \right)^2}{n} \right)^{1/2} \tag{3}$$

where n is the number of patterns, y_{nn} the network prediction, $y_{\exp}$ the experimental response and i is an index of the data. The most important step in the development of the ANN model is the selection of the optimum number of hidden layer neurons in the ANN architecture.

Though hidden layers do not directly interact with the external environment, they have a great effect on the final target. Both the number of hidden layers and the number of neurons in hidden layers must be carefully considered. The topologies used to determine the optimal number of hidden layer neurons showed that the number of these neurons varied from 2 to 12. It was found that the best performance of the network is obtained with eight neurons are in the hidden layer.

During the training, the whole sample set (27 runs) was divided for training, validation, and testing in 70:15:15 proportions. The regression coefficient (R^2) is a measure of the explanatory power of the model. Here for the best predictive model chosen values of R^2 is 0.999, 0.992 and 0.981 for training, validation, and testing respectively as shown in Fig. 13. The overall predicted R^2 for the model was 0.991 as shown in Fig. 13, indicating the quality of the trained network and its high predictability.

3.5. Comparison of the ANN and RSM models

Response surface methodology and artificial neural network have been widely applied in optimizing and modelling various processes in environmental studies.

RSM consists of a collection of statistical and mathematical techniques for designing experiments, modelling,

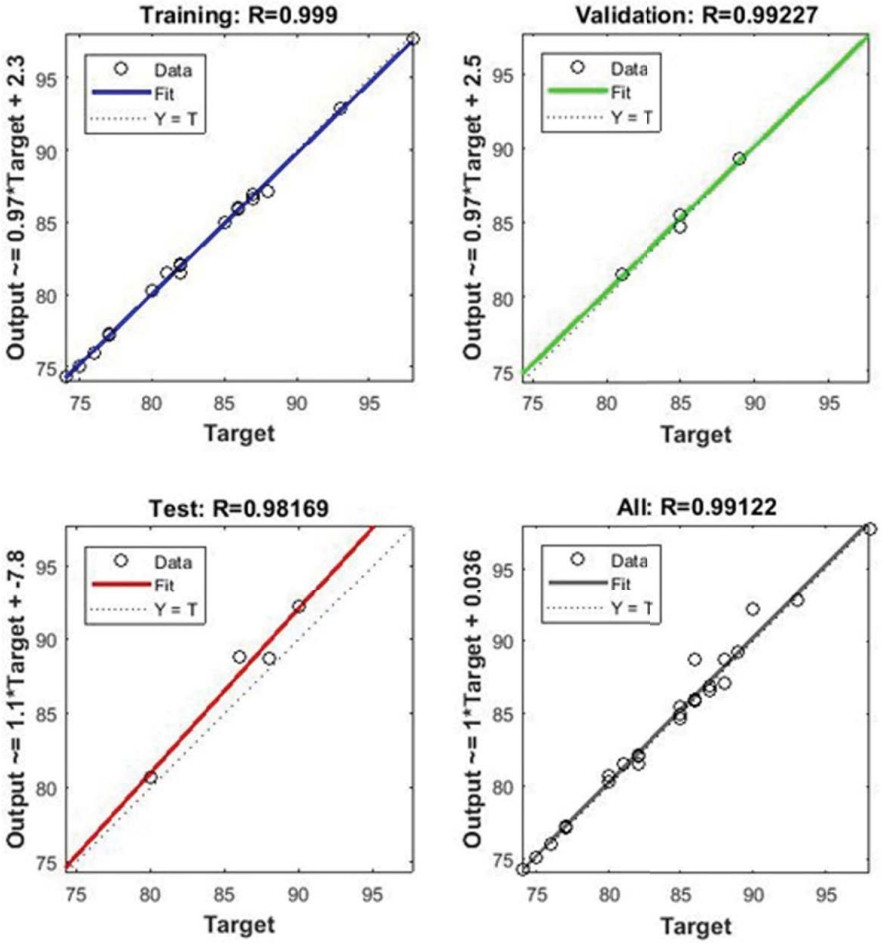

Fig. 13. Neural network model with training, validation, test and all prediction set.

evaluating the effects of factors and searching for the optimum condition [26].

The main advantage of RSM is the ability to reduce the number of experiments and determine the contribution of each factor in predicted response due to the accurate statistical analysis.

This ability is powerful in identifying the insignificant main parameters and interaction or quadratic terms in the model and thereby can reduce the complexity of the issue.

On the other hand, this technique can be used only within certain ranges of parameters, which are selected before the modelling. ANN has developed as an attractive tool for nonlinear multivariate modelling [27]. The main advantages of ANN are: (i) ANN can learn from observing data sets and (ii) ANN can inherently capture almost any complex and non-linear process.

Therefore, the ANN model is so predictable and flexible that new experimental data can be added to build a reliable model. The comparative values of MSE and R^2 are given in Table 6.

4. Conclusions

Fe_3O_4@MgAl-LDH as a new magnetic catalyst for wet peroxide oxidation of phenol from wastewater was developed and promising activity resulted.

The main advantages of the magnetic nanocomposite were the low price of the nanocomposite, high activity, and easy removal after the process. The process was modelled and optimized by both response surface methodology and artificial neural network. The Pareto analysis indicated that phenol concentration is the most important factor in the CWPO process. Besides, the interaction between catalyst amount and peroxide volume was the most significant effecting parameter on the efficiency of phenol remediation. The optimum condition was at 0.5 L^{-1}, 100 min, 0.7 mL, 65.15 ppm of catalyst amount, reaction time, peroxide volume and phenol concentration, respectively. Under these optimized conditions, the experimental degradation of phenol (98%) agreed with the predicted response value (around 97%). The ANN model showed the superior capability to the RSM model with a mean square error of 0.22 and a regression coefficient of 0.99. The study indicates that the application of magnetic layered double hydroxides in the removal of phenolic wastewater could be promising and further studies are under study.

References

[1] N.A. Yusoff, S.-A. Ong, L.-N. Ho, Y.-S. Wong, W.F. Khalik, Degradation of phenol through solar-photocatalytic treatment by zinc oxide in aqueous solution, Desal. Water. Treat., 54 (2014) 1621–1628.

[2] B.-J. Zhou, T.-H. Chen, Biodegradation of phenol with chromium(VI) reduction by the *Pseudomonas* sp. strain JF122, Desal. Water Treat., 57 (2016) 3544–3551.

[3] S.A. Hosseini, M. Davodian, A.R. Abbasian, Remediation of phenol and phenolic derivatives by catalytic wet peroxide oxidation over Co-Ni layered double nano hydroxides, J. Taiwan Inst. Chem. Eng., 75 (2017) 97–104.

[4] A. Hussain, S.K. Dubey, V. Kumar, Kinetic study for aerobic treatment of phenolic wastewater, Water Resour. Ind., 11 (2015) 81–90.

[5] A. Dargahi, M. Mohammadi, F. Amirian, A. Karami, A. Almasi, Phenol removal from oil refinery wastewater using anaerobic stabilization pond modeling and process optimization using response surface methodology (RSM), Desal. Water Treat., 87 (2017) 199–208.

[6] A. Almasi, A. Dargahi, A. Amrane, M. Fazlzadeh, M. Soltanian, A. Hashemian, Effect of molasses addition as biodegradable material on phenol removal under anaerobic conditions, Environ. Eng. Manage. J., 17 (2018) 1475–1482.

[7] R. Shokoohi, H. Movahedian, A. Dargahi, A. Jonidi Jafari, A. Parvaresh, Survey on efficiency of BF/AS integrated biological system in phenol removal of wastewater, Desal. Water Treat., 82 (2017) 315–321.

[8] R. Shokoohi, R. Azami Gillani, M. Molla Mahmoudi, A. Dargahi, Investigation of the efficiency of heterogeneous Fenton-like process using modified magnetic nanoparticles with sodium alginate in removing Bisphenol A from aquatic environments: kinetic studies, Desal. Water Treat., 101 (2018) 185–192.

[9] L.G. Cordova Villegas, N. Mashhadi, M. Chen, D. Mukherjee, K.E. Taylor, N. Biswas, A short review of techniques for phenol removal from wastewater, Curr. Pollut. Rep., 2 (2016) 157–167.

[10] S.W. Zhou, C.T. Gu, Z. Qian, J.G. Xu, C.H. Xia, The activity and selectivity of catalytic peroxide oxidation of chlorophenols over Cu–Al hydrotalcite/clay composite, J. Colloid Interface Sci., 357 (2011) 447–452.

[11] X.M. Tao, D. Liu, J.J. Song, Q.G. Ye, D.Y. Xu, Plasma modification of ZnMgAl-LDHs for adsorption property improvement, J. Taiwan Inst. Chem. Eng., 74 (2017) 281–288.

[12] P. Koilraj, K. Srinivasan, High sorptive removal of borate from aqueous solution using calcined ZnAl layered double hydroxides, Ind. Eng. Chem. Res., 50 (2011) 6943–6951.

[13] C.P. Chen, P. Gunawan, R. Xu, Self-assembled Fe_3O_4-layered double hydroxide colloidal nanohybrids with excellent performance for treatment of organic dyes in water, J. Mater. Chem., 21 (2011) 1218–1225.

[14] R.-X. Wang, T. Wen, X.-L. Wu, A.-W. Xu, Highly efficient removal of humic acid from aqueous solutions by Mg/Al layered double hydroxides–Fe_3O_4 nanocomposites, RSC Adv., 4 (2014) 21802–21809.

[15] M.F. Shao, F.Y. Ning, J.W. Zhao, M. Wei, D.G. Evans, X. Duan, Preparation of Fe_3O_4@SiO_2@layered double hydroxide core–shell microspheres for magnetic separation of proteins, J. Am. Chem. Soc., 134 (2012) 1071–1077.

[16] Z. Rezvani, M. Sarkarat, Synthesis and characterization of magnetic composites: intercalation of naproxen into Mg-Al layered double hydroxides coated on Fe_3O_4, J. Inorg. General Chem., 638 (2012) 874–880.

[17] S. Christoskova, M. Stoyanova, Degradation of phenolic waste waters over Ni-oxide, Water Res., 35 (2001) 2073–2077.

[18] A.I. Khuri, J.A. Cornell, Response Surface: Design and Analysis, Marcel Dekker Inc., New York, 1987.

[19] M. Rajasimman, P. Karthic, Application of response surface methodology for the extraction of chromium(VI) by emulsion liquid membrane, J. Taiwan Inst. Chem. Eng., 41 (2010) 105–110.

[20] D.M. Himmelblau, Applications of artificial neural networks in chemical engineering, Korean J. Chem. Eng., 17 (2000) 373–392.

[21] P. Koilraj, K. Sasaki, Fe_3O_4/MgAl-NO_3 layered double hydroxide as a magnetically separable sorbent for the remediation of aqueous phosphate, J. Environ. Chem. Eng., 4 (2016) 984–991.

[22] W. Tongamp, Q. Zhang, F. Saito, Preparation of meixnerite (Mg–Al–OH) type layered double hydroxide by a mechano-chemical route, J. Mater. Sci., 42 (2007) 9210–9215.

[23] O. Gholipoor, S.A. Hosseini, Phenol removal from wastewater by CWPO process over the Cu-MOF nanocatalyst: process modeling by response surface methodology (RSM) and kinetic and isothermal studies, New J. Chem., 45 (2021) 2536–2549.

[24] R. Shokoohi, A. Joneidi Jafari, A. Dargahi, Z. Torkshavand, Study of the efficiency of bio-filter and activated sludge (BF/AS) combined process in phenol removal from aqueous solution: determination of removing model according to response surface methodology (RSM), Desal. Water Treat., 77 (2017) 256–263.

[25] A. Azizi, A. Dargahi, A. Almasi, Biological removal of diazinon in a moving bed biofilm reactor – process optimization with central composite design, Toxin Rev., 9 (2019) 1–11.
[26] S.A. Hosseini, O. Gholipoor, Removal of arsenic from aqueous solutions using $MgFe_2O_4$ nano spinel and GO/$MgFe_2O_4$ nanocomposite: an application of response surface methodology, Desal. Water Treat., 89 (2017) 162–170.
[27] U. Özdemir, B. Özbay, S. Veli, S. Zor, Modeling adsorption of sodium dodecyl benzene sulfonate (SDBS) onto polyaniline (PANI) by using multilinear regression and artificial neural networks, Chem. Eng. J., 178 (2011) 183–90.